EGYPTIAN DENTAL JOURNAL

Vol. 64, 2171:2182, July, 2018

I.S.S.N 0070-9484

Oral Medicine, X-Ray, Oral Biology and Oral Pathology

www.eda-egypt.org • Codex : 64/1807

OSTEOCONDUCTIVITY OF TWO NOVEL BIODEGRADABLE MAGNESIUM ALLOYS (ZK30A&ZK10A) FOR REPAIRING BONE DEFECT IN DOGS

Heba A. Shalaby*, Nesrine khairy** *and* Marwa Sameer Moussa ***

ABSTRACT

Background: Magnesium alloys containing zinc and zirconia are promising alloys as biodegradable orthopedic replacement bone

The objective: of this research was to evaluate of the ability of ZK30A and ZK10A Mg-alloys as biodegradable alloplastic bone substitute for bone formation of adequate quality and quantity in repairing bony defects in femoral shaft of dogs.

Materials and Methods: A total of eight skeletally mature mongrel male dogs with an average age 20 ± 2-month-old and weighing 15-18 kg were used in this study. The dogs divided into two groups, group I; contains 8 dogs with type I (ZK30A) alloy plates implanted in holes made in upper right femoral shaft and group II contains the same 8 dogs with type II (ZK10A) alloy plates implanted in holes made in lower right femoral shaft. The quantitative and qualitative assessments of newly formed bone tissue were carried out and assessed by In vivo radiography, scanning electron microscope and EDX for elemental analysis.

Results: radiographic results of bone density of group I showed high bone resorption after three weeks implantation, followed by high rate of bone formation after 6 weeks, then regressed to bone resorption again, finally after 12 weeks bone deposition again insignificant with those at 6 weeks. Whereas group II showed normal pattern of bone resorption till six weeks, followed by bone formation till the end of experiment. Both types of alloys showed bone resorption first after implantation, but they differed in longevity and severity of initial bone resorption; group I was severe for three weeks whereas group II was less in severity for six weeks.. Scanning electron microscopic results of both magnesium alloys (group I and group II)_3 months post-implantation showed new bone formation. Type I(ZK30A) alloys induced new bone in approximate contact to implanted alloy surface. Whereas, type II (ZK10A) alloys induced new bone in close intimate contact and well integrated with implanted alloy surface EDX for elemental analysis of the newly formed bone showed non-significant difference between group I and group II in calcium, Ca/P ratio and zinc.

* Associate Professor, Dental Biomaterial Department, Faculty of Dentistry, Alfyoum University, Egypt.
** Lecturer of Oral Surgery, Faculty of Dentistry, Cairo University, Egypt.
*** Lecturer of Oral Biology, Faculty of Dentistry, Cairo University, Egypt.

Conclusion: Both Mg-Zn-Zr alloys are liable to form qualified mineral bone. The pattern of osteointegration is directly related to the biodegradation rate and stable corrosive products formation. Mg Zn alloy with higher Zr (ZK10A) showed lower biodegradation tendency and high susceptibility for new bone integrated with orthopedic implant. Mg Zn alloy with lower Zr (ZK30A) showed higher biodegradation tendency and encouraged new bone formation with wide gap distance. ZK10A is promising osteoconductive biodegradable implant.

KEYWORDS: Biodegradable Mg-Zn-Zr Alloys, bone substitute, Osteoconduction, osseointegration, peri-implant new bone formation.

INTRODUCTION

Bone is a natural living tissue which is composed of 50-70% mineral, 20-40% organic matrix, 5 to 10% water, and <3% lipids. [1]. Bone mineral allows mechanical rigidity and load-bearing strength, while the organic matrix offers elasticity and flexibility to bone [2] which is susceptible to fracture due to trauma or pathological lesion [3]. Bone defect heals spontaneously in good physiological conditions due to the renewal capacity of bone. Though, large defects, or critical bone defects, may not rebuild naturally due to decreased blood supply, opposed wound environment, metabolic factors, hormones, and applied stress. Alloplastic materials used in bone repair is classified into bio-inert, biodegradable materials [4], and considered osteoconductive which allow bone growth on its surface and acts as a scaffold for the surrounding cells and tissue to invade, grow and thus help new bone formation. [5] The most clinically successful is the bio-inert materials but they need a second surgical procedure for removal, therefore, research has been required for biodegradable bone substitutes which can be used as an implant and do not require a second surgery for removal. [5,6].

Magnesium (Mg) based alloys can be defined as novel generation of bio-metals suitable for fixation of bone fracture [7]. Magnesium plays a major role in mineral homeostasis of bone [8], has mechanical properties similar to natural bone and have the potential to serve as osteoconductive biodegradable implants for load-bearing applications. [9,10]

Numerous publications concluded that magnesium alloys promote bone attachment to implant surfaces compared to conventional materials. [11,12]

Degradation of magnesium can cause the loss of mechanical integrity in a short period which can limit its application as an implant material [13]. Moreover, evolution of hydrogen gas bubbles accompanied by the rapid degradation of magnesium delay bone healing [14] so alloying Mg with Si, Zn, Ca, and Zr could improve the strength and decrease degradation rate of magnesium alloys to allow sufficient bone repair. [15,16]

Recently, new Mg-alloy systems were developed by adding Zinc (Zn) and Zirconia (Zr) on the expanse of Mg element, as ZK30A and ZK10A to be used as biodegradable orthopedic implants. Zinc is one of the most essential nutrient elements in the human body, it is present in all organs, tissues, fluids and body secretions and 86% of zinc is present in the muscles and bones [17]. Zinc plays an important role in bone formation, mineralization and preservation of bone mass [18]. Zn ions released from the implant during the degradation phase without producing systemic toxic side effects [19] and reduce hydrogen gas evolution during biodegradation [20]. Zirconia is usually used in Mg alloys containing Zinc as Zr is a powerful grain refiner for Mg alloys [21] and addition of 1% Zr in Mg alloys resulted in reduction of the degradation rate by 50 % and significant improvement of the ductility of the alloy [22].

The objective of this research was to evaluate of the ability of ZK30A and ZK10A alloys as biodegradable alloplastic bone substitute for bone formation of adequate quality and quantity.

MATERIALS AND METHODS

Experimental Animals:

All study procedures were done in accordance to and approved by the "Institutional Animal Care and Use Committee (IACUC)" of faculty of Veterinary

Medicine, Cairo University. A total of eight skeletally mature mongrel male dogs with an average age 20 ± 2-month-old and weighing 15-18 kg were used in this study. Each dog was given a complete clinical, physical and radiographic examination to exclude the evidence of systemic, orthopedic, and neurologic disease. Dogs were housed individually in separate cages at the department of Veterinary Surgery, Anesthesiology and Radiology, Faculty of Veterinary Medicine, Cairo University. Before enrollment in the study, dogs were quarantined for two weeks; kennels were sprayed with 6/1000 ml Neocidal diazinone, dogs were bathed in 1/1000 ml Neocidal diazinone and Ivermectine was injected in a dose of 0.1 mg/kg body weight subcutaneously to guard against ecto-parasitic and endo-parasitic infestation. The dogs divided into two groups, group I; contains 8 dogs with type I (ZK30A) alloy plates implanted into holes made in upper right femoral shaft and group II; contains the same 8 dogs with type II (ZK10A) alloy plates implanted into holes made in lower right femoral shaft.

Surgical Procedures:

Animal preparation:

The animals were fasted 12 hours prior to surgery and allowed the free access to drinking water till the time of anesthesia. The animal was prepared in lateral recumbency with the right side uppermost. The cephalic vein was cannulated using a 20 G I.V. canula. The skin over the right pelvic limb from dorsal midline to the tarsal joint was circumferentially prepared for aseptic surgery. The hair coat was clipped and shaved, washed with water and soap then painted with 10% Povidone-Iodine.

Anesthetic protocol:

1. Premedication

Dogs were premedicated with Atropine sulfate subcutaneously 10-30-minuts before induction of anesthesia in a dose of 0.05 mg/kg weight and tranquilized with xylazine HCL 1mg/kg body weight intramuscular.

2. Induction of anesthesia

Ketmine HCL was used for anesthetic induction in a dose 5mg/kg body weight intravenous via the cephalic catheter. Anesthesia was maintained during the operative time by venous drip (½ g thiopental /500ml dextrose 5%) with a drip rate 28-40 drops/ minute [23]**.** Dogs were intubated to keep the respiratory airway patent by the use of endotracheal tube.

Surgical exposure of the femur:

A lateral approach to the right femur was done with accordance to ***Piermattei and Johnson,***[24] The skin was incised at the whole length of the femur. The skin edges were reflected to expose the fascia lata, which was incised along the line of its attachment to the biceps femoris to reveal the vastus lateralis muscle that was bluntly separated together with the biceps femoris by blunt dissection and retracted to expose the shaft of the femur.

Implants fixation:

The two Mg-alloys (ZK30A&ZK10A) plates sample were inserted into the right femoral shaft of the dogs in upper and lower part.

TABLE (1) Chemical composition of investigated Mg alloys as supplied by manufacturer

Composition	Mg type I (ZK30A)	Mg type II (ZK10A)
Elements	Wt%	Wt%
Mg	96.42	98.15
Zn	2.86	1.15
Zr	0.41	0.55
Si	0.1	0.1
V	0.09	0.03
Nb	0.02	0.02

Abbreviations: ***Mg, magnesium, Zn; zinc, Zr.: zirconia, Si: silicon, wt.: weight.***

After complete exposure of the femur, one hole was drilled in the upper extremity of the right femur to receive one plate for group I. The osteotomy site was gradually enlarged by using successive drillers 2, 2.5, 3, 3.5 mm at 800 rpm respectively to the full

length of 10mm for socket creation. The drilling procedure was performed with low speed under copious irrigation to prevent bone overheating and washing bone debris. The same procedures were repeated in the lower extremity of the femur for another plate for group II. During placement, the implants were press fit into the osteotomy sites by gentle manual pressure. Finally, the surgical site was irrigated with saline mixed with gentamycin. The wound layers were repositioned and sutured using absorbable suture material Vicryl 1-0.

Post-operative care

Dogs were kept in separate cages, fed with standard diet and activity was limited to leash walking during the study. Doges received course of broad spectrum antibiotic cefotax 1mg/12 hours for 7 days. All dogs were subjected to daily clinical examination, including evidence of infection, local reaction and regional lymph node enlargement.

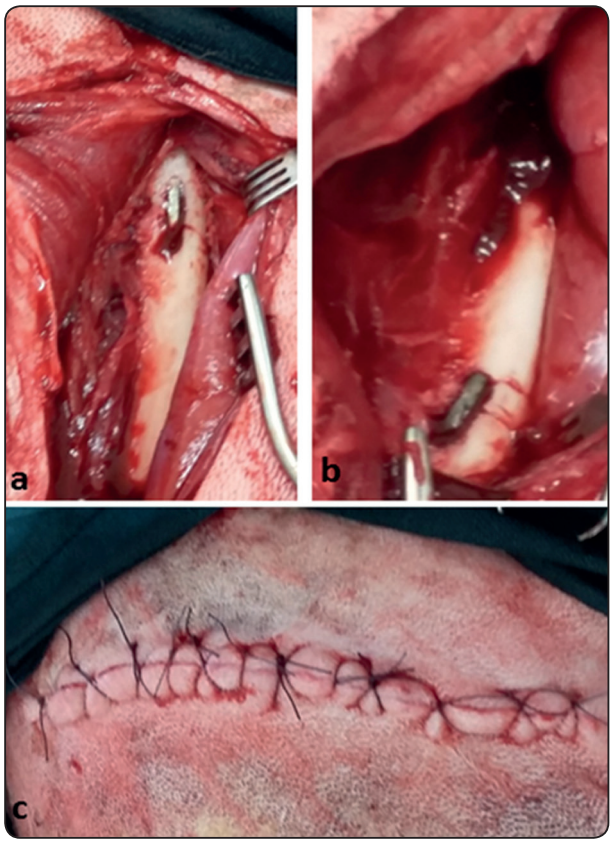

Fig. (1) Photographs showing a): the prepared place with group I plate inserted in the upper part of the right femur. b): the prepared place with group II plate inserted in the lower part of the right femur. c): the closure of the wound with vicryl 1-0.

Post Operative Assessments:

Radiographic examination

An orthogonal radiographic projection (medio-lateral) was made immediately post-operative, 3, 6, 9 and 12 weeks post-operative. (Figure 2) An aluminum step wedge was always used for standardization. It was necessary to convert the radiographs into digital form for further qualitative /quantitative image analysis. For determination of the bone density, densitometric Digora software (Orion Corp. Sordex medical system, Finland) was used to measure the mean density.

Bone density determined by software of the four lines mesially and distally was recorded and then the mean value was calculated. Finally, these readings were compared to the other intact side in each bone's Dogs. As well, bone density of each line was compared with the corresponding value of aluminum step wedge (two successive steps); Figure (3). Then, the bone density was calculated according to the following equation:

The obtained data of bone density were collected, tabulated and statistically analyzed.

Euthanasia:

The experimental animals were euthanized twelve weeks after samples implantation surgery by an overdose of thiopental. The skin was reopened by blunt dissection and the bone with the implant was removed as block and immersed in 10% formalin.

Bone specimens (size of ~1 cm3) from the peri-implant area from all animals were excised and fixed in 10% buffered formaldehyde at 4°C for a period of 3 days. After fixation the specimens were dehydrated in increasing grades of isopropyl

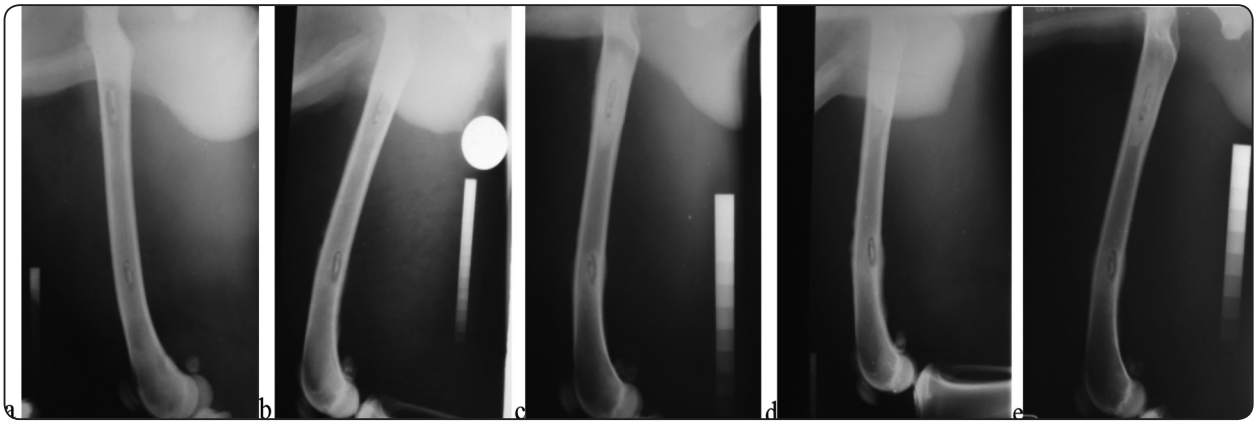

Fig. (2) Postoperative medio-lateral radiographs of the right femur showing upper part group I and lower part group II; a) immediate post-operative, b) 3weeks post-operative, c) 6weeks post-operative, d) 9weeks post-operative, e) 12weeks post-operative.

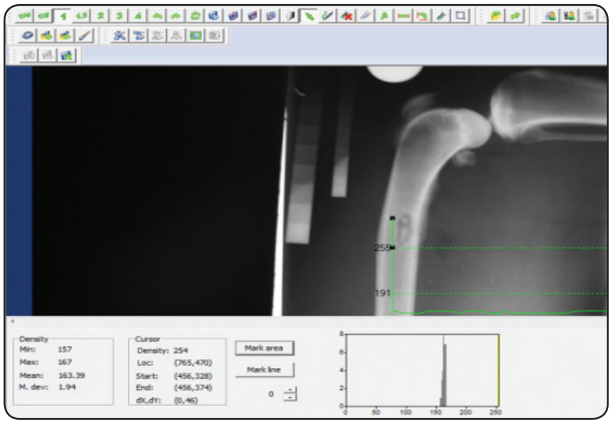

Fig. (3) Determination of bone density using Digora system. (Thickness of step 1-x)/ (Thickness of step 2) = (Density of step 1-density of bone (line reading))/ (Density of step 1-density of step 2)

alcohol (70%, 80%, 95%, 100%) and cleared with xylene. The samples were embedded in methyl-methacrylate and, to facilitate complete infiltration of the bone tissue with the embedding medium, cold polymerization of methyl-methacrylate was done with specimens at 4°C for 3 days. Benzoyl peroxide was used as initiator, and final polymerization was done with N-N Dimethyl-p-toluidine as accelerator. Sections of 10 μm thickness of each specimen were cut using a saw microtome Leica SP1600 (Leica Microsystems, Wetzlar, Germany) in the perpendicular plane to the implant surface (sagittal sections). Each bone was cut into eight to 12 sagittal sections through the marrow region, depending on their thickness and three sections from each bone were used for Scanning Electron Microscopy and EDX.

Assessment of the Newly Formed Bone:

The morphology of newly formed bone was examined by using SEM, (Quanta 250 FEG -Field Emission Gun- attached, Netherlands). Each specimen was sputtered coated with gold palladium and thus became ready for scanning with different magnifications. Elemental analysis was performed to quantify the different elements and normal stoichiometric composition of ca/p ratio of HA crystals of newly formed bone by using Energy Dispersive X-ray (EDAX).

Statistical analysis:

Data presented as mean, standard deviation (SD). Repeated measure ANOVA were used to compare between different tested groups and follow-up period for % of bone density followed by pairwise comparison with Bonferroni correction. For elemental analysis, Independent t-test used to compare between tested groups. significance level was set at $P \leq 0.05$. The Statistical analysis was performed with IBM® SPSS® (SPSS Inc., IBM Corporation, NY, USA) Statistics Version 25 for Windows.

RESULTS

Clinical observations:

In the first few days after surgery, the dogs showed normal postoperative appearance of a relatively slight wound swelling and reddening. All clinical signs resolved within 1 week after surgery and the animals regained full weight-bearing use of the implanted leg without any clinical signs for local inflammatory reactions or wound dehiscence through the follow-up period.

Radiographic Observations:

In group I there was statistical significant reduction in mean bone density at 3weeks post-operative (4.73±0.63), followed by statistical significant increase in mean bone density at 6weeks post-operative (7.77±1.03). At 9weeks post-operative there was statistical significant decrease in mean bone density (4.46± 0.75) and it was followed by statistical significant increase at 12weeks post-operative (7.91±0.99). Comparing the mean bone density at 12weeks post-operative with the immediate post-operative, there was statistical significant decrease. Table (2) and figure (4).

In group II there was non-statistical significant decrease in mean bone density at 3weeks post-operative (7.28±1.56), followed by statistical significant decrease in mean bone density at 6weeks post-operative (4.82±0.59). At 9weeks post-operative there was statistical significant increase in mean bone density (7.45±1.54) and it was followed by non-statistical significant decrease at 12weeks post-operative (7.34±1.63). Comparing the mean bone density at 12weeks post-operative with the immediate post-operative, there was non-statistical significant decrease. Table (2) and figure (4).

Osseointegration assessment during healing period:

The statistical analysis and test of significance of the densitometrical measurements of the newly formed bone around the differently implants surfaces in the experimental animals presented in Table (2) and Figure(4). The radiographic examination of implant area of group I during the follow up period, and after bone density analysis showed typical bizarre shape in bone remodeling, Group I showed high bone resorption after three weeks implantation, followed by high rate of bone formation after 6 weeks, then regressed to bone resorption again, finally after 12 weeks bone deposition again insignificant with those at 6 weeks. Whereas group II showed normal pattern of bone resorption till six weeks, followed by bone formation till the end of experiment. Both types of alloys showed bone resorption first after implantation, but they differed in longevity and severity of initial bone resorption; group I was severe for three weeks whereas group II was less in severity for six weeks.

TABLE (2) Mean and standard deviation (SD) for Bone density changes of newly formed bone among the studied groups at different time intervals (immediate, 3, 6, 9 and 12 weeks) in experimental Dogs.

Time intervals Bone density	Group I		Group II		p-value
	Mean	SD	Mean	SD	
Immediate	9.06[a]	0.82	7.77[a]	0.73	0.009*
3ws	4.73[c]	0.63	7.28[a]	1.56	0.002*
6ws	7.77[b]	1.03	4.82[b]	0.59	≤0.001*
9ws	4.46[c]	0.75	7.45[a]	1.54	0.001*
12ws	7.91[b]	0.99	7.34[a]	1.63	0.445 NS
p-value	≤0.001*		0.001*		

sMeans with the same lowercase letter within each column is not significant at p≥0.05

****= Significant, NS=Non-significant.***

SEM results

Scanning electron microscopic results of both Mg alloys (ZK30A & ZK10 A) showed new bone formation after 3 months post-implantation. The newly formed trabecular bone showed concentric bone lamellae with intervening lacunae of osteocytes. Group I (ZK30A) alloys induced new bone in approximate contact to implanted alloy surface. Wide gap spaces were observed between the new bone and the implant surface.(Figures 5)

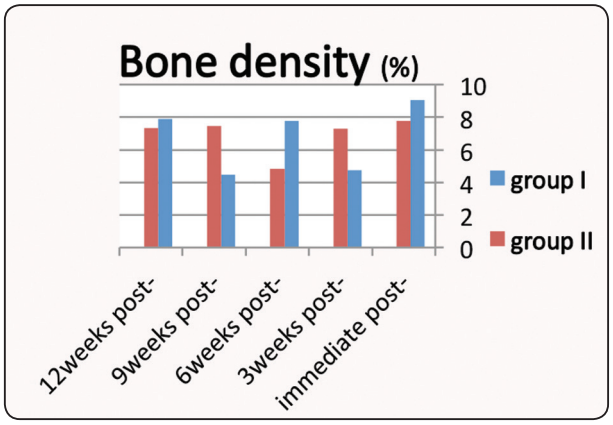

Fig. (4) Mean % of bone density for group I and group II throughout the experiment.

Whereas, group II (ZK10A) alloys induced new bone in close intimate contact and well integrated with implanted alloy surface. Reduced gap spaces were observed. (Figures 6).

The surface of the implanted alloy showed surface irregularities, roughness and cracks, (Figures 5, 6).

Wide gap spaces were observed and recorded between the new bone and the implant surface, about (143.5 μm) in group I. Reduced gap spaces were observed and recorded between the new bone and the implant surface; about (6.8 μm) in group II. (Figure7)

The surface corrosion irregularities and cracks were less in aggressiveness and more homogeneous than alloy group I, (Figure7).

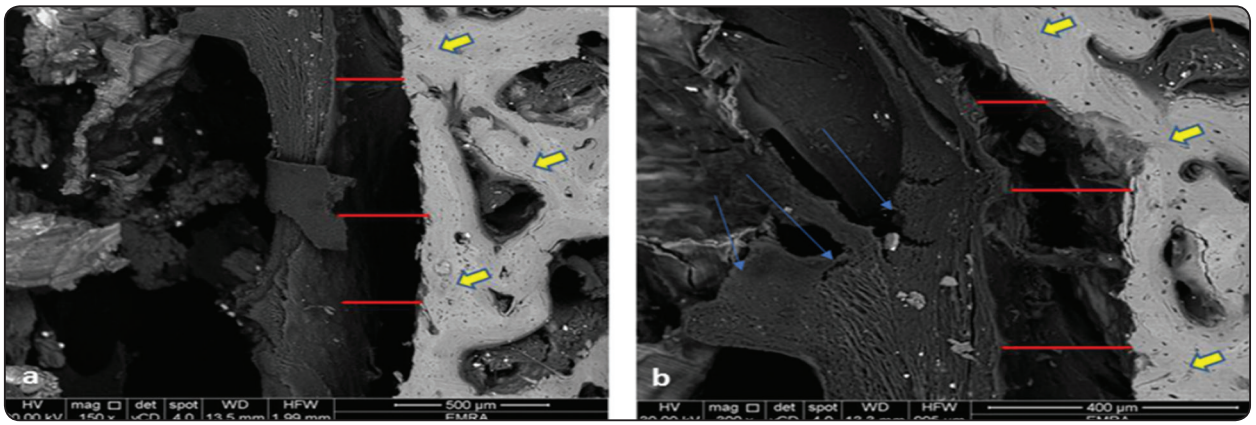

Fig. 5 (a,b): Scanning electron micrograph of group I Mg alloy (ZK30A); showing:new bone formation with concentric lamellae (trabeculae) of bone and intervening lacunae of osteocyte (yellow arrows). gap distance spaces between the newly formed bone and the implant alloy (red lines). Surface implant corrosive areas (blue arrows).

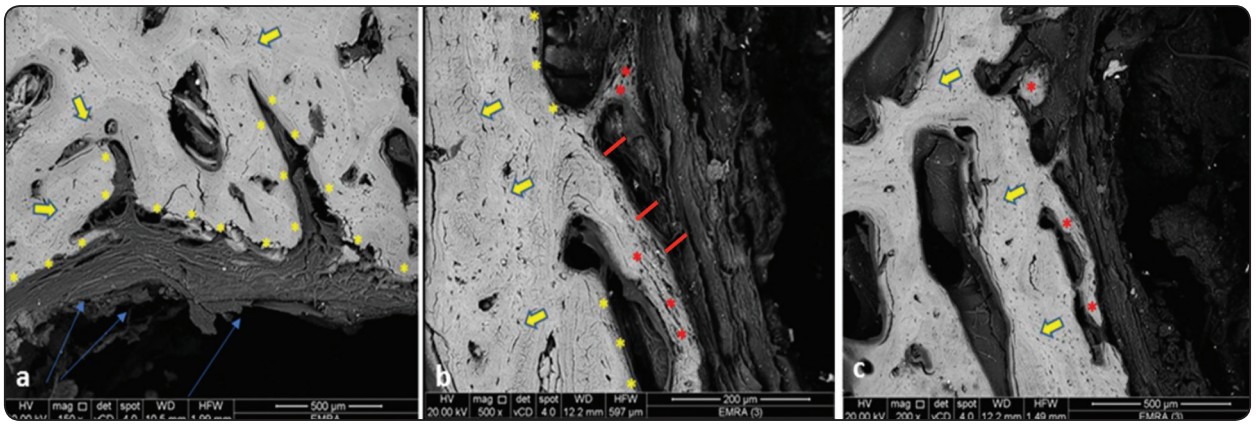

Fig. (6) (a,b,c): Scanning electron micrograph of group II Mg alloy (ZK10A); showin:new bone formation with concentric lamellae (trabeculae) of bone and intervening lacunae of osteocyte (yellow arrows). Areas of bone formation on the surface of the implant alloy (red stars). gap distance spaces between the newly formed bone and the implant alloy (red lines). Surface implant corrosive areas (blue arrows)

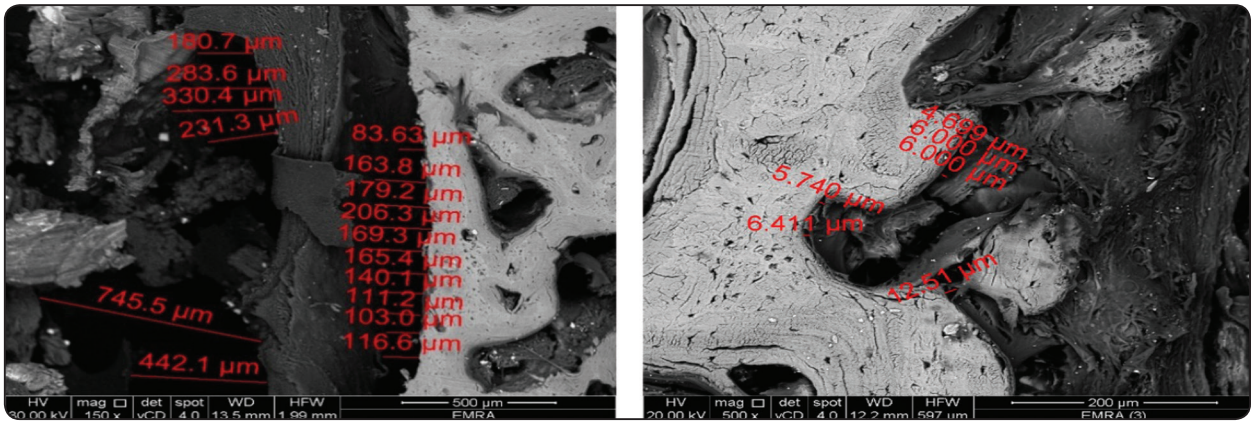

Fig. (7a) Scanning electron micrograph of group I Mg alloy (ZK30A); showing; gap distance spaces between the newly formed bone and the implant alloy (red lines). These spaces about (143.5 µm). The surface corrosion irregularities and cracks were more in aggressiveness and less homogeneous than alloy group II. Fig. (7a) Scanning electron micrograph of group II Mg alloy (ZK10A); showing; gap distance spaces between the newly formed bone and the implant alloy (red lines). These spaces about (6.8 µm). The surface corrosion irregularities and cracks were less in aggressiveness and more homogeneous than alloy group I.

Elemental analysis (EDXA):

The statistical data for elemental analysis of newly formed bone around and replacing the both implanted alloys groups I and II by using EDXA are shown at Table (3).

The statistical data recorded significant increase in O,Zn, Zr and Mg elements than group II than group I (31.06±3.87,2.40± 2.98, 0.98±0.36, 3.55±1.87) and (29.29±0.89,0.52±0.12, 0.66±0.01, 1.38±0.56), respectively. On the other hand, group I alloy revealed significant increase in phosphorous elements than group II; (17.61±0.26,14.37±3.97) respectively. group I recorded slight non-significant increase in Ca element amount than group II in (36.74±2.09, 30.63±8.85).

Ca/P ratio for the new bone formed around both types of implant alloys revealed non-significant different ratio with Ca/P ratio of normal bone.

The newly formed bone around type II alloy showed slight non significant increase in Ca/P ratio than type I . Ca/P ratio for type II alloy is 2.13±0.04 and for type I is 2.09±0.13. Ca/P ratio for normal bone is 2.3±0.03. table (4).

TABLE (3) Mean and standard deviation (SD) for different element analysis.

	Group I (ZK30A)		Group II (ZK10A)		p-value
	Mean	SD	Mean	SD	
O	29.29	0.89	31.06	3.87	0.198 *
Zr	0.66	0.01	0.98	0.36	0.019*
Mg	1.83	0.56	3.55	1.87	0.017*
P	17.61	0.26	14.37	3.97	0.026*
Ca	36.74	2.09	30.63	8.58	0.055 NS
Zn	0.52	0.12	2.40	2.98	0.068 *

= Significant, NS=Non-significant***

TABLE (4) Mean and standard deviation (sd) for Ca/P ratio for newly formed bone and normal bone.

	Group I (ZK30A)		Group II (ZK10A)		Normal bone		p-value
	Mean	SD	Mean	SD	Mean	Sd	
Ca/P	2.09	0.13	2.13	0.04	2.3	0.02	0.361 NS

DISCUSSION

Mg alloys containing zinc and zirconia are promising alloys as biodegradable orthopedic replacement bone [7].

The stability of biodegradable implants plays a vital role in determining the biological quality of osseous regeneration of endosseous prostheses [1]. It is of great importance for the biodegradable implants to induce sufficient bone of high quality around itself before the implant decomposes. In large bone defects; the biodegradation rate of implant should be synronized with qualified bone formation. The in-vitro studies for corrosion rate of Mg alloys are not enough to assure and explain the in-vivo behavior in human. Hence animal experimental trials for newly developed biodegradable Mg-alloy is essential. Animal in- vivo evaluation becomes mandatory to understand how the implant will behave in human bone under normal physiological environment and determine the quality of osseous regeneration.[25].

Our work has mainly focused on in vivo study of two novel Mg alloys (ZK30A and ZK10A) in femur bones of dogs. Dogs were used in this study as animal model, as they are known to maintain uniformity in their genetic characteristics. They have comparable organ sizes in relation to humans, which made them ideal for the study [26].

For assessment of bone formation in vivo, the two most important properties of implant-induced new bone tissue are osteoconduction and osteointegration. These two processes were evaluated by radiographic examination and scanning electron microscopic examination of peri-implant bone sections.

The clinical observation after surgical implantation of both types of alloy and during the experiment period indicated positive and healthy signs of normal healing.

In the current work, the radiographic examination and bone density analysis of group I alloy showed high bone resorption after three week implantation, followed by high rate of bone formation after 6 weeks, then regressed to bone resorption again. Finally after 12 weeks bone deposition again which was insignificant with those at 6 weeks. Whereas group II showed normal pattern of bone resorption till six weeks, followed by bone formation till the end of experiment.

Both groups showed bone resorption after implantation for both types of alloys, but they differed in longevity and severity of initial bone resorption.

In type I alloy, bone resorption was severe for three weeks whereas in type II alloy, it was less in severity for six weeks.

The initial bone resorption is normal reaction after implantation, this might be attributed to inflammatory response after surgery. Stimulation of inflammatory cells synchronized with osteoclastic activity leading to decrease in the pH of cellular media surrounding the implant and consequently bone resorption. Aggressive bone resorption with group I alloy was clearly detected due to its high bio-corrosion susceptibility. [27]

Mg alloys mainly consist of ά-Mg matrix and β-eutectic compounds along the grain boundaries and within grains. Eutectic compounds precipitates are Zr-Zn containing particles. Type II alloy has Zn and Zr higher in percent than type I alloy, so its Eutectic compound was precipitated at higher amount than type I. β-eutectic compounds act as a cathode whereas ά-Mg matrix as anode led to developing of galvanic corrosion [28].

The β-eutectic compounds act as barrier zone against corrosion progressing[29].

Higher percentage of Zr elements in group II alloys lead to decrease galvanic corrosion than group I alloy.

Galvanic corrosion led to more dissolution of Mg ions from implant surface to extracellular fluid, enhanced formation of more corrosive products Mg(OH)2 and MgO. The two compounds Mg $(OH)_2$

and MgO will be precipitated according to equation (1&2). This is in accordance to [27]

$$Mg \leftrightarrow Mg+ + e \quad (1)$$

$$Mg+2 + H2O \rightarrow Mg+2 + OH- + \tfrac{1}{2} H2 \quad (2)$$

This step was accompanied by H ion evolution. H ions development was concentrated at vicinity to α-Mg matrix, consequently more pitting and corrosion was enhanced. Evolution of hydrogen bubbles enhanced and encouraged cell death and bone resorption.[14]

Furthermore, the mineralization and bone formation were encouraged in alkaline media. $Mg(OH)_2$ in high amount enhance alkalinity and further calcium phosphate deposition. This is accompanied by more attraction of osteoblasts and more bone formation [30]. This explains the high rate of bone formation in group I after six weeks .

In group II alloy, the nature and amount of deposited and precipitated phases encouraged the deposition of more stable minerals and bone on implant surface with high integration mechanism. This mechanism was continuous with slow rate, so the increased density was obvious after nine weeks. Bone formation continue developing with constant rate, assured by our results.

The surface degradation of both implanted alloys was accompanied by deposition of passive compounds that suppress further degradation. Mg $(OH)_2$, MgO and β-eutectic phase were increased with increased Zn and Zr percent in (group II). $Mg(OH)_2$ and MgO are considered the initial nuclei for crystallization and growth of calcium phosphate of HA crystal [30].

According to equations number 3 & 4, it was obvious that group II alloy have more mineralization than group I, hence the density of bone in group II was higher in our study.

$$Mg^{2}+ + Ca^{2+} + HPO^{4-} \rightarrow Mg_xCa_y(PO_4)_z \quad (3)$$

$$10\ Ca^{2+} + 6PO_4^{3-} + 2OH^{-} \rightarrow Ca_{10}(PO_4)_6(OH)_2 \quad (4)$$

Whereas type I implant surface revealed high rate of degradation that exceed bone formation process. As wide defects and cracks were developed over the implant surface that enhanced further degradation and more hydrogen bubbles evolutions with their adverse effect on living cells and bone formation[14]. Adding to that, decrease pH led to unstable and soluble calcium phosphate precipitations. Hence group I showed decreased in density after nine weeks. In the present study, group I showed precipitation of corrosive products with calcium phosphate layer deposition which reversed the pH again to be alkaline and new growth of calcium phosphate mineral. Hence bone density after twelve weeks increased again to be non-significant with those at six weeks.

In the present work, the radiographic examination resuts are in line with scanning electron microscopic results. Our scanning electron microscopic results showed new bone formation for both Mg alloys (ZK10 A& ZK30A). The newly formed trabecular bone showed concentric bone lamellae with intervening lacunae of osteocyte.

In group I, bone was developed apart from implant surface with wide gap distance areas to implant surface about (143.5 μm). Whereas group II implant surface reduced gap distance areas about (6.8 μm) and the new bone integrated with implant surface. This can be linked to the high degradation rate of type I alloy that exceeded rate of bone formation .

From histological point of view group II (ZK10A) implant induced new bone formation on the surface of the implant itself. The osteoblasts secrete a collagen-rich bone matrix directly on the implant surface as they differentiated into osteocytes. In later stages, the matrix was mineralized as calcified collagen. This is in accordance with Davies JE [31]. Furthermore, elemental analysis of newly formed bone around implant revealed high significant amount of Mg in group II implants. Increasing Mg level enhanced osteogenic differentiation of stem cells with inhibitory effects on osteoclast function. [32]

On other hand, group I (ZK30A) implant showed new bone with a space between the new bone and the implant surface. The new bone was not formed on the implant surface as in group II.

The mineral quality of newly formed bone around implants was assessed by Ca/P ratio analysis that was compared with normal ratio of bone of dog. Both types of implant alloys revealed non-significant different ratio with normal bone. This means that the mineral bone quality was not affected by the type of Mg alloy selected in this study.

CONCLUSIONS

Under the limitations of the present investigation the following conclusion can be drawn:

1. Both Mg-Zn-Zr alloys are liable to form qualified mineral bone.
2. The pattern of osteointegration is directly related to the biodegradation rate and stable corrosive products formation.
3. Mg Zn alloy with higher Zr (ZK10A) showed lower biodegradation tendency and high susceptibility for contact ossteogesis integrated with orthopedic implant.
4. Mg Zn alloy with lower Zr (ZK30A) showed higher biodegradation tendency and encouraged bone osteogenesis with wide gap distance.
5. ZK10A is promising osteoconductive biodegradable implant.

ACKNOWLEDGEMENTS

The authors express their sincere thanks to Prof. Dr. Ing. Bohuslav MASEK, University of West Bohemia in Pilsen, Czech Republic, EU. for providing the alloys. Prof Dr Aiad: Faculty of Veterinary Medicine for the surgical procedure .

Central Metallurgical Research and Development Institute, Cairo, Egypt for providing the lab Facilities for work.

REFERENCES

1. Athanasiou, K.A.; Zhu, C.; Lanctot, D.R.; Agrawal, C.M.; Wang, X. Fundamentals of biomechanics in tissue engineering of bone. Tissue Eng. 2000,6,361–381.
2. Driessens, F.C.; van Dijk, J.W.; Borggreven, J.M. Biological calcium phosphates and their role in the physiology of bone and dental tissues I. Composition and solubility of calcium phosphates. Calcif. Tissue Res. 1978, 26, 127–137.
3. Cavalcanti, S.C.; Pereira, C.L.; Mazzonetto, R.; de Moraes, M.; Moreira, R.W. Histological and histomorphometric analyses of calcium phosphate cement in rabbit calvaria. J. Cranio Maxillo Facial Surg. 2008, 36, 354–359. .
4. Yeung, K.W.; Wong, K.H. Biodegradable metallic materials for orthopaedic implantations: A review. Technol. Health Care 2012, 20, 345–362.
5. Frost HM (1989). The biology of fracture healing. An overview for clinicans, part II. Clin Orthop Rel Res 248: 294–309.
6. Wuisman, P.I.; Smit, T.H. Bioresorbablepolymers: Heading for a new generation of spinalcages. Eur. Spine J. 2006, 15, 133–148.
7. Li Z., Gu X., Lou S. & Zheng Y. The development of binary Mg-Ca alloys for use as biodegradable materials within bone. Biomaterials 29, 1329–1344 (2008).
8. Del Barrio RA, Giro G, Belluci MM, Pereira RM, Orrico SR. Effect of severe dietary magnesium deficiency on systemic bone density and removal torque of osseointegrated implants. Int J Oral Maxillofac Implants. 2010;25:1125–1130.
9. Zheng Y. F., Gu X. N. & Witte F. Biodegradable metals. Mat Sci Eng R 77, 1–34 (2014).
10. Staiger MP[1], Pietak AM, Huadmai J, Dias G.: Magnesium and its alloys as orthopedic biomaterials: a review. Biomaterials. 2006 Mar;27(9):1728-34. Epub 2005 Oct 24.
11. Cecchinato F, Karlsson J, Ferroni L, Gardin C, Galli S, Wennerberg A, Zavan B, Andersson M, Jimbo R. Osteogenic potential of human adipose-derived stromal cells on 3-dimensional mesoporous TiO2 coating with magnesium impregnation. Materials Science and Engineering: C. 2015,52:225-234.
12. Castellani C, Lindtner RA, Hausbrandt P, Tschegg E, Stanzl-Tschegg SE, Zanoni G, Beck S, Weinberg, AM. Bone-implant interface strength and osseointegration: biodegradable magnesium alloy versus standard titanium control. Acta Biomater. 2011,7:432–440. 9.

13. Niemeyer M. Magnesium Alloys as Biodegradable Metallic Implant Materials. Proceedings of 7th Conference on Advanced Materials and Processes; Rimini, Italy. 2001.
14. Song, G.-L. and Song, S.-Z. "Corrosion Behavior of Pure Magnesium in a Simulated Body Fluid", Acta PhysicoChimica, 2006; 22(10), pp. 1222-1226.
15. González S, Pellicer E, Fornell J, Blanquer A, Barrios L, Ibañez E, Solsona P, Suriñach S, Baró MD, Nogués C, Sort J. Improved mechanical perfomance and delayed corrosion phenomena in biodegradable Mg-Zn-Ca alloys through Pd-alloying. Journal of the Mechanical Behavior of Biomedical Materials 2012; 6: 53-62.
16. Sheikh, Z.; Javaid, M.A.; Hamdan, N.; Hashmi, R. Bone regeneration using bone morphogenetic proteins and various biomaterial carriers. Materials 2015, 8, 1778–1816.
17. Plum, L.M.; Rink, L.; Haase, H. The essential toxin: Impact of zinc on human health. Int. J. Environ. Res. Public Health 2010, 7, 1342–1365.
18. Murni, N.; Dambatta, M.; Yeap, S.; Froemming, G.; Hermawan, H. Cytotoxicity evaluation of biodegradable Zn–3Mg alloy toward normal human osteoblast cells. Mater. Sci. Eng. C 2015, 49, 560–566.
19. Liu, X.; Sun, J.; Qiu, K.; Yang, Y.; Pu, Z.; Li, L.; Zheng, Y. Effects of alloying elements (Ca and Sr) on microstructure, mechanical property and in vitro corrosion behavior of biodegradable Zn–1.5Mg alloy. J. Alloys Compd. 2016, 664, 444–452.
20. R Radha and D Sreekanth : Insight of magnesium alloys and composites for orthopedic implant applications – a review.: Journal of Magnesium and Alloys Volume 5, Issue 3, September 2017, Pages 286-312.
21. Tsai MH, Chen MS, Lin LH, Lin MH, Wu CZ, Ou KL, Yu CH: Effect of heat treatment on the microstructures and damping properties of biomedical Mg–Zr alloy. J Alloys Compounds 509, 813–819 (2011)
22. Zhang W, Li M, Chen Q, Hu W, Zhang W, Xin W: Effects of Sr and Sn on microstructure and corrosion resistance of Mg–Zr–Ca magnesium alloy for biomedical applications. Mater Des 39, 379–383 (2012)
23. Asbury AJ, Tzabar Y. Fuzzy-logic new ways of thinking for anesthesia. Br J Anaesth 1995; 75(1):1-2
24. Piermattei DL, Johnson KA. (2004a) Approach to the craniodorsal and caudodorsal aspects of the hip joint by tenotomy of the gluteal muscles. In: Piermattei DL, Johnson KA (eds), An Atlas of Surgical Approaches to the Bones and Joints of the Dog and Cat (4th edn). Philadelphia: Saunders, pp. 306e308.
25. Dolly Mushahary, Ragamouni Sravanthi, Yuncang Li, Mahesh J Kumar, Nemani Harishankar, Peter D Hodgson, Cuie Wen, and Gopal Pande: Zirconium, calcium, and strontium contents in magnesium based biodegradable alloys modulate the efficiency of implant-induced osseointegration: Int J Nanomedicine. 2013; 8: 2887–2902.
26. Tsai KL, Clark LA, Murphy KE: Understanding hereditary diseases using the dog and human as companion model systems. Mamm Genome.2007; 18(6-7):444-51.
27. Heba A. Shalaby and Madiha M. Shoeib.: BIO-DEGRADATION OF Mg-ALLOY CONTAINING Zn AND Zr FOR ORTHOPEDIC APPLICATION E.D.J. Vol. 62, No. 4, 66-80, 2016.
28. 28-Park. B. K., Jun. J. H. and Kim. J. M., "Influence of Zn Addition on Aging Response and Corrosion Resistance of Mg-Gd-Nd-Zr Alloy". Materials Transactions, 2008; 49: 5, 931 – 935.
29. Song G.L. and Atrens A.: Understanding magnesium corrosion—A framework for improved alloy performance. Adv. Eng. Mater. , 2003; 5, 837.
30. Janning C[1], Willbold E, Vogt C, Nellesen J, Meyer-Lindenberg A, Windhagen H, Thorey F, Witte F. Magnesium hydroxide temporarily enhancing osteoblast activity and decreasing the osteoclast number in peri-implant bone remodelling. Acta Biomater. 2010 May;6(5):1861-8.
31. Davies JE. Understanding peri-implant endosseous healing. J Dent Educ. 2003;67(8):932–949.
32. Ma J., Thompson M., Zhao N. & Zhu D. H. Similarities and differences in coatings for magnesium-based stents and orthopaedic implants. JOT 2, 118–130 (2014).